The International Journal of Advanced Manufacturing Technology (2019) 105:4989–5008
https://doi.org/10.1007/s00170-019-04436-0

ORIGINAL ARTICLE

Optimization analysis considering the cutting effects for high-speed five-axis down milling process by employing ball end mill

Xiaoxiao Chen [1,2] · Jun Zhao [2] · Wenwu Zhang [1]

Received: 29 December 2018 / Accepted: 20 September 2019 / Published online: 16 November 2019

Abstract
As one of the advanced manufacturing technologies, high-speed five-axis ball end milling has been widely used in high-end manufacturing fields because of its high efficiency, high quality, and high precision. Based on the analysis of cutting effect and response surface methodology, a series of experiments were carried out. Based on geometric modeling and numerical simulation, various tool postures are comprehensively analyzed, and the down milling process combining positive tilt angle and positive lead angle can achieve better cutting effect. The variance and interaction of the important factors affecting the surface integrity and the cutting process were analyzed, and the polynomial equations reflecting the relationship between the processing index and the input process variable were obtained. Finally, a process optimization schemes with various optimization criteria were proposed. When using a larger *tilt*, smaller f_z and higher spindle rotation speed for multi-objective optimization, a combination of a smaller a_p and a smaller a_e, or a combination of a larger a_p and a smaller a_e is advantageous to result in high ideality. The combinations of large *lead*, large *tilt*, and high spindle speed give full play to the advantages of high-speed cutting technology. The process optimization plan will help determine the processing strategy for achieving the desired machining results and better surface quality based on actual application requirements. Finally, the future research areas are prospected for the high-performance machining technology.

Keywords Tool postures · Surface quality · Cutting effects · Process optimization

1 Introduction

Multi-axis ball end milling is widely used in aerospace, automotive, and die and mold industries for complex surface machining [1]. Due to technical superiority, high-speed cutting has been applied in many manufacturing fields [2]. The combination of high-speed cutting and multi-axis machining can promote the technological progress and engineering application of high-end manufacturing. Because H13 has excellent comprehensive mechanical properties and high-temperature tempering stability as a hot work die steel, it is widely used [3].

The relative postures between tool and workpiece during the machining process significantly influence the cutting effects and surface integrity for multi-axis milling operation. Material processing in different postures can be achieved by setting the relative position and angle between the workpiece geometry and the machining tool path [4–8], or by adjusting the tool vector for multi-axis machining operations [9–11]. Different processing postures produce different effective cutting speeds and material removal modes, which have a significant impact on processing quality and effects. Some published papers studied the effects of relative postures between the tool and workpiece on the machining process, tool wear, tool life, and machined surface integrity [4–8, 11].

Toh [4] investigated the three-dimensional surface topography of ball end milling of inclined workpieces at 75° in various tool path directions. Daymi et al. [5] concluded that workpiece angle 25° produced the best surface finish when inclined end milling Ti–6Al–4V, and also surface damage layer, heat effect, and white interface layer are limited or not

✉ Xiaoxiao Chen
chenxiaoxiao@nimte.ac.cn

[1] Ningbo Institute of Materials Technology and Engineering, Chinese Academy of Sciences, Ningbo, Zhejiang 315201, China

[2] Key Laboratory of High Efficiency and Clean Mechanical Manufacture of MOE, School of Mechanical Engineering, Shandong University, Jinan 250061, Shandong, China

found, which shows the advantages of inclined milling. By studying the influence of workpiece inclination on the processing quality, Axinte and Dewes [6] found that the surface roughness decreases and also the compressive stress is lower due to the lack of friction effect caused by the center of ball end mill when the inclination angle of 60° workpiece angle is used. Mhamdi et al. [7] focused on the different machining postures at different tool positions, and the participation of the cutting edges is achieved by the movement of the tool along the contour of the concave surface, and found that surface roughness and microhardness are sensitive to the relative posture at different tool positions, which proves the relative machining angles are a critical parameter to improve surface quality. Denkena et al. [9] established the stochastic surface topography model for ball end milling of TiAl6V4, and lead angle of 15° that could reduce the scallop height produced by feed per tooth and step-over was used. Pu and Singh [8] studied the tool wear and surface integrity of ball end milling with three different tool materials under the condition that the workpiece was tilted by 45° for hardened AISI A2 tool steel, which could introduce favorable effective cutting speed. When ball end milling with varying milling directions and workpiece angles, Aspinwall et al. [11] found that the cutting forces significantly decrease under horizontal downwards milling condition using a workpiece tilt angle of 45° when compared with the condition when milling with the workpiece tilt angle 0°.

With regard to five-axis machining, tool orientation plays an important role in the resulting cutting process and the machined surface integrity that significantly affects the performance of the machined parts. The modeling of cutting force that is related to tool wear, tool life, tool deformation, machining vibration, etc. has been a hot topic of research [1, 12–14], which will further affect surface quality. There are many factors affecting the vibration of machining. Vibration research of five-axis machining system involves dynamics and stability [15, 16]. For mechanism analysis, finite element method is generally used in machining process simulation, which could analyze the change of physical quantity in the processing action area [17]. On the premise of ensuring the smooth and controllable processing process, the optimization of tool axis posture based on motion analysis can give full play to the kinematics advantages of five-axis machining [10, 18, 19]. Surface quality directly serves engineering applications, is the final output of the five-axis processing system, and has a key impact on the performance of components. Its evaluation mainly includes surface roughness, surface topography, hardness, microstructure, residual stress, etc., and there are many factors influencing surface quality. Researchers have done some works on this, and analyzed the mechanism and law of the influence of tool relative postures on the machined surface integrity [9, 11, 20–23].

Zhang [13] optimized the machining process by changing the feed rate with the variation of tool-workpiece contact condition along the tool path based on the modeling of the cutting forces. Tool orientation adjustment with motion constraints is valuable for multi-axis machining, especially for high-speed machining [18, 19], which could provide better stability of cutting speed and tool orientation or makes best use of the kinematic characteristics of angular feed. Kalvoda and Hwang [20] studied the influence of tool inclination angle on the surface integrity with regard to low carbon steel, and the results showed that tilt angle presented primary influence on the surface integrity.

In actual machining, the space posture of the tool axis vector with respect to the feed direction is various, and the machining characteristics and mechanism of using the compound tool inclination needs to be further clarified. Chen et al. [21–23] investigated the effects of various single or compound inclination angles on tool-working characteristics and surface quality of multi-axis ball end milling of hardened steel. In addition, process optimization for the compound tool inclination angles still needs to be advanced for practical machining application. In general, multi-objective optimization, such as Taguchi-based gray relational analysis, particle swarm optimization, and response surface method, is a common method for predicting processing results [24–26].

However, the published works on process optimization especially considering machined surface and cutting effects were limited. It is critical to conduct process optimization for high-speed multi-axis ball end milling in order to achieve better processing efficiency, quality, and accuracy. Through geometric analysis, experimental research, numerical simulation, and response surface multi-objective optimization method, the interaction between process parameters, especially tool inclination and various tool postures optimization, was studied in this work.

2 Analysis of the tool-workpiece action zone

For machining of specific geometrical features, the accessibility of the cutter should be considered, and the tool postures continually vary during the machining process. All the tool inclination angles relative to the normal direction of the machined point could be divided into eight types, as is shown in Fig. 1. The definition of tilt angle and lead angle in multi-axis ball end milling process could refer to the works [21]. It is necessary to study the effects of tool postures on the cutting effects and seek optimal compound inclination angles with high ideal degree. Different tool orientations result in different tool tip positions, postures of the engaged cutting edges, and effective cutting speeds, which lead to the variations of the characteristics of cut in and cut out of single cutting flute and material removal performance. Further, the differences in cutting heat, mechanical load, and energy consumption generated during the multi-axis milling process would be induced.

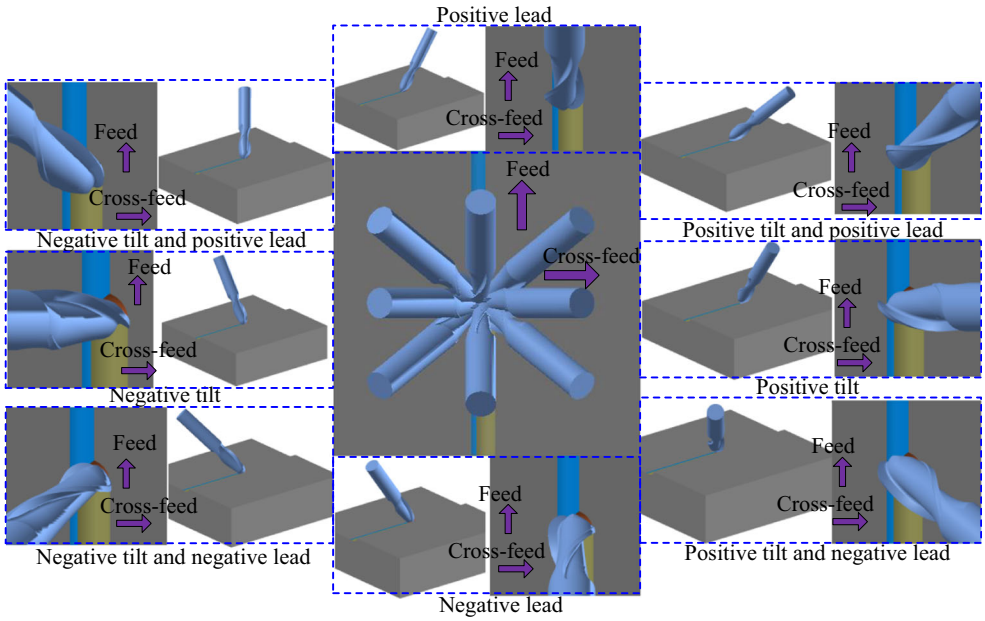

Fig. 1 Different tool postures under down milling condition

Finally, the machined surfaces with different geometrical features and physical and mechanical properties were generated.

Based on the finite element modeling method [17], the cutting temperature field corresponding to *tilt* 16° was present in Fig. 2, and the approximate semicircular temperature field and the temperature field of the slightly curly chip during the chip separation process could be observed obviously. Each part of the cutting edge section has different cutting speed, and the workpiece material deformation intensity changes along the engaged cutting edges, which is reflected in the temperature difference in different tool-workpiece contact area positions.

The instantaneous workpiece temperature fields for chip separation corresponding to *tilt* − 24° and *lead* − 24° during cutting process of single cutting flute are shown in Fig. 3. The temperature fields of the workpiece corresponding to the working condition of different tool angles present an approximate annular decreasing temperature circle. The maximum temperature of the workpiece at the moment of chip separation at *tilt* − 24° is slightly higher than the maximum temperature of the workpiece at the working condition at the *lead* − 24°, and the shape of the temperature field determined by the spatial motion posture of the cutting edge segment under different tool inclination angles is different.

Comprehensively analyzing the eight types of tool postures, the tool tip moves away from the tool-workpiece contact area under positive *tilt*, positive *lead*, and combinations of positive *tilt* and positive *lead*, and also the corresponding effective cutting speed is high. The material removal characteristics are also ideal under positive *tilt*, positive *lead*, and combinations of positive *tilt* and positive *lead*, and the chip could be smoothly removed along the chip pocket without

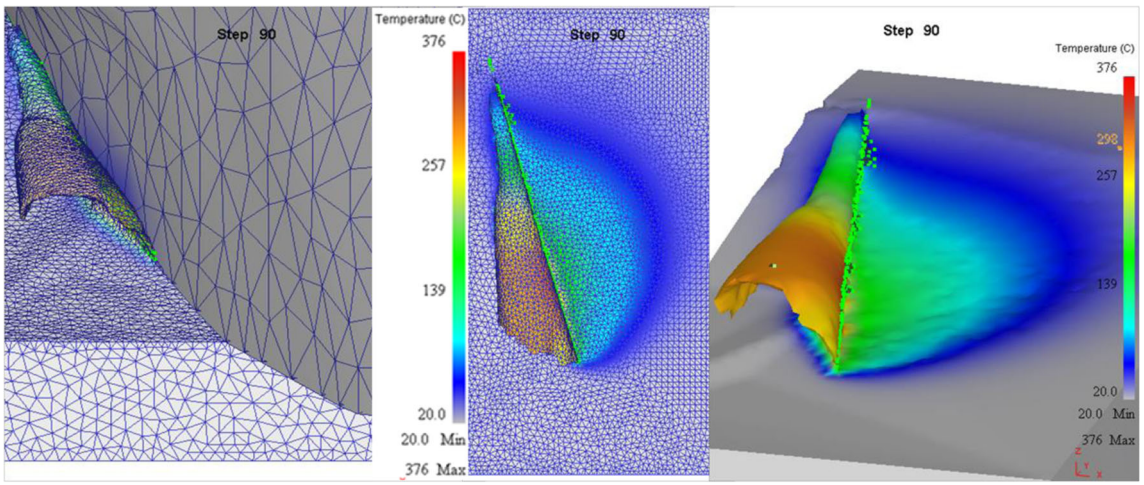

Fig. 2 Cutting temperature fields corresponding to *tilt* 16°

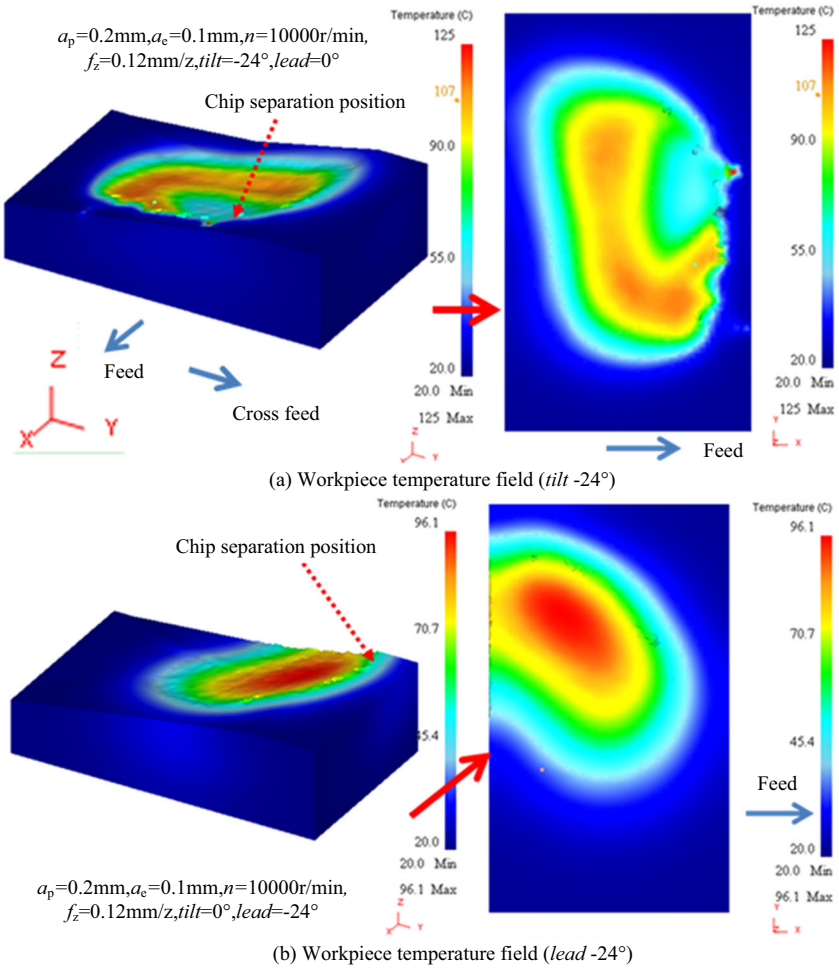

Fig. 3 The instantaneous workpiece temperature fields for chip separation corresponding to *tilt* − 24° and *lead* − 24°

squeezing the final machined surface especially when adopting combinations of positive *tilt* and positive *lead*. The different views for compound inclination angle with positive *tilt* and positive *lead* are presented in Fig. 4. This research works mainly concentrate on the effects of the preferred compound inclination angles that are concluded by optimization analysis on the cutting process and surface quality.

3 Experimental details

Systematic experiments were carried out in a five-axis machining center. The hardened H13 die steels and the solid carbide ball end mill with a diameter of 10 mm were used. The machined surface geometry was measured by an optical profilometer (model: Veeco NT9300). The surface hardness was measured using a Leeb hardness tester (Model: HL-600), and the average value of the three measured results was used to evaluate the surface quality. The cutting forces were detected by Kistler 9257B measurement system. The machining and detection system is presented in Fig. 5. In the experiments, a specific area of about 10 × 10 (mm × mm) was processed according to a certain combination of technological parameters. Hundreds of thousands and even more measured points were sampled in the detection area, and then statistical analysis was carried out to obtain the surface roughness Ra, Rq, and Rt, which is general and can eliminate random errors. The surface roughness index is an area parameter.

The Design Expert software was used to design B Box-Behnken response surface experiments, and the test points are taken at the midpoint of the edge of the cube. The method has the following characteristics: firstly, the number of test is less than the design of the central composite test when the number of factors is identical; there are no combinations that simultaneously arrange all the test factors to a high level of test, which is especially used for tests with safety requirements or special needs; it has an approximate rotation type, and there is no sequential nature. The process parameters are determined according to the matching attribute between tool and workpiece material together with the recommended reasonable selection of applied parameters by the tool manufacturer. For high-speed finish machining, the relatively large material removal rate has been applied in the experiments. When designing the process plans, the feed per tooth is taken as one of the

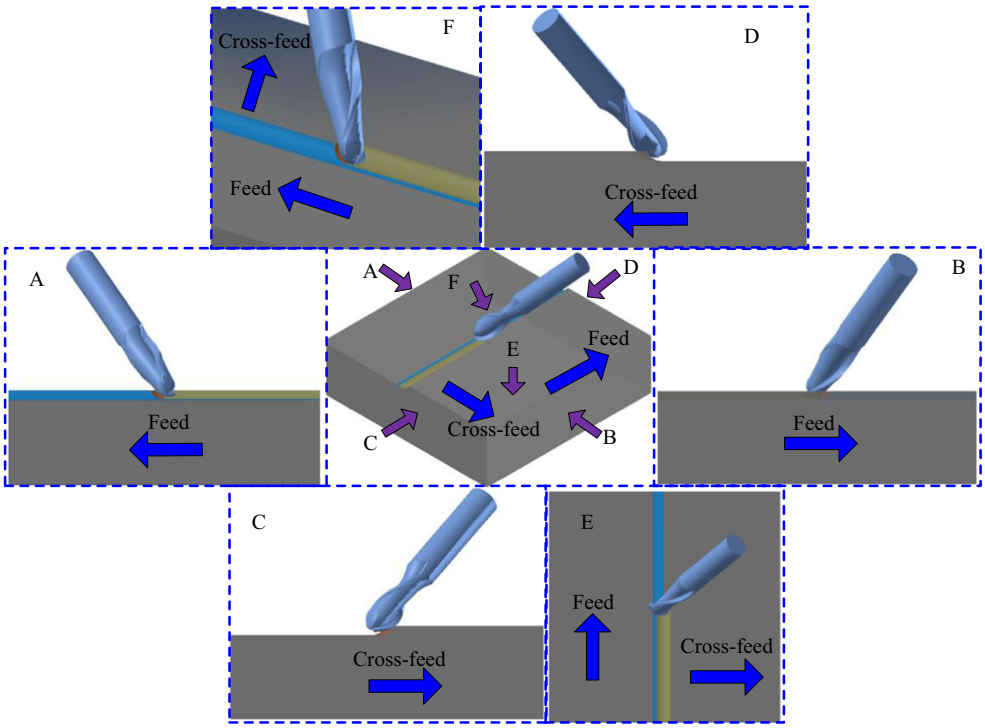

Fig. 4 Diagrams for compound inclination angle with positive *tilt* and positive *lead* from different views

consideration criteria to increase the MMR, and larger feed per tooth values that is matching the high rotation speed of spindle were applied in the milling process. The values of depth of cut and width of cut are also in a larger numerical range in order to obtain high materials' removal rates. In addition, the research work belongs to the field of high-speed machining technology according to the determined high spindle rotation speed. The overall conclusion is favorable for high-speed and high-quality finish machining operations.

According to the previous theoretical discussion and experimental conclusions [22], combinations of positive *tilt* and positive *lead* help to produce better cutting effects and ideal

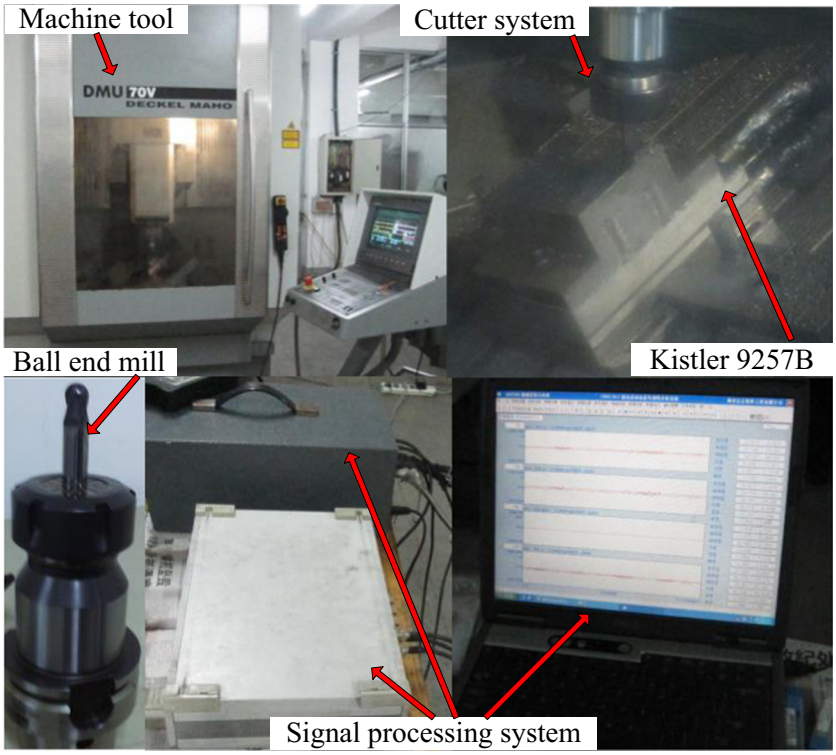

Fig. 5 Diagram of the machining and detection system

surface quality for down milling. Multiple-factor response surface experiment were designed, and fifty-four sets of experiments with preferred tool orientation angles were carried out under down milling conditions. The process parameters shown in Table 1 are controlled within a specific range. The *tilt* and *lead* are set within the range from 10° to 40°, and dry cutting with gas cooling condition was applied. The symbols of a_p, a_e, n, and f_z are depth of cut, width of cut, spindle speed, and feed per tooth, respectively. The maximum spindle speed and cutting speed of the ball end mill can reach 13000 r/min and 408.2 m/min, which is at the high-speed cutting range.

Based on the geometric modeling analysis, numerical simulation technology, the experimental design was conducted. A five-axis machining center, dynamometer, and data acquisition equipment were used during the machining process, and the machined surface geometry and surface hardness were detected by white light interferometer and hardness tester.

The interaction of various factors on cutting effect (maximum and average cutting force) and the influence of the surface geometry, surface hardness, were analyzed, and the single objective and multi-objective coupling optimization process considering the cutting effect and surface integrity were carried out. The corresponding flow chart is shown in Fig. 6.

4 Response and optimization of geometrical indicators

The spatial posture and position of the engaged cutting edges in ball end mill cutter are determined by the tool inclination angles, movement parameters, and geometrical process parameters, and the final surface topographies could be observed in different views with various distribution of surface area unit, as is shown in Fig. 7. The sampled surface roughness is around 0.7 μ. In general, the surface features are primarily determined by the relative spatial movement of the engaged cutting edge under specific process parameters and the uncut material on the workpiece. In addition, there are also influencing factors such as vibration, deformation, and eccentricity. The smallest surface roughness is easy to be obtained by adopting small width of cut, moderate depth of cut, moderate feed speed, large tilt angle, and small lead angle when high-speed milling of hardened steel.

In this work, the influence of significant technological factor interaction on the corresponding evaluation index system was analyzed and discussed, and the 3D response surfaces of the evaluation index that reflects the change regularities of the evaluation index with the variation of the process parameters were determined. It can be found that the ideal evaluation index, such as the minimum surface roughness, will appear in specific combinations of process parameters under some conditions. At the same time single-objective process optimization and multi-objective coupling optimization are carried out, the ideal process optimization schemes which provides important technological

Table 1 Detailed process parameters settings for down milling

Number	a_p/ mm	a_e/ mm	n/ (r/min)	f_z/(mm/ z)	*tilt*/ °	*lead*/ °
1	0.35	0.25	13000	0.2	25	40
2	0.35	0.4	10000	0.35	40	25
3	0.35	0.25	10000	0.5	25	10
4	0.35	0.25	11500	0.35	25	25
5	0.5	0.4	11500	0.5	25	25
6	0.2	0.25	13000	0.35	25	40
7	0.35	0.4	11500	0.35	10	10
8	0.2	0.4	11500	0.5	25	25
9	0.5	0.25	11500	0.5	10	25
10	0.5	0.25	11500	0.5	40	25
11	0.35	0.25	10000	0.2	25	10
12	0.35	0.4	10000	0.35	10	25
13	0.35	0.1	11500	0.35	40	40
14	0.2	0.25	11500	0.5	10	25
15	0.2	0.25	11500	0.2	40	25
16	0.5	0.25	10000	0.35	25	10
17	0.5	0.25	11500	0.2	10	25
18	0.5	0.4	11500	0.2	25	25
19	0.2	0.1	11500	0.2	25	25
20	0.35	0.25	11500	0.35	25	25
21	0.35	0.1	10000	0.35	40	25
22	0.2	0.1	11500	0.5	25	25
23	0.35	0.4	11500	0.35	10	40
24	0.35	0.4	11500	0.35	40	10
25	0.35	0.1	13000	0.35	40	25
26	0.35	0.4	13000	0.35	10	25
27	0.35	0.25	13000	0.2	25	10
28	0.5	0.25	11500	0.2	40	25
29	0.2	0.25	10000	0.35	25	10
30	0.2	0.25	11500	0.2	10	25
31	0.35	0.1	11500	0.35	40	10
32	0.35	0.25	10000	0.5	25	40
33	0.5	0.1	11500	0.2	25	25
34	0.35	0.25	13000	0.5	25	40
35	0.35	0.25	11500	0.35	25	25
36	0.35	0.1	13000	0.35	10	25
37	0.35	0.1	11500	0.35	10	40
38	0.5	0.25	13000	0.35	25	40
39	0.35	0.25	11500	0.35	25	25
40	0.35	0.25	10000	0.2	25	40
41	0.35	0.25	13000	0.5	25	10
42	0.35	0.25	11500	0.35	25	25
43	0.35	0.1	11500	0.35	10	10
44	0.2	0.4	11500	0.2	25	25
45	0.5	0.1	11500	0.5	25	25
46	0.2	0.25	11500	0.5	40	25
47	0.35	0.4	11500	0.35	40	40
48	0.2	0.25	10000	0.35	25	40

Table 1 (continued)

Number	a_p/ mm	a_e/ mm	n/ (r/min)	f_z/(mm/ z)	*tilt*/ °	*lead*/ °
49	0.35	0.25	11500	0.35	25	25
50	0.5	0.25	10000	0.35	25	40
51	0.5	0.25	13000	0.35	25	10
52	0.35	0.4	13000	0.35	40	25
53	0.2	0.25	13000	0.35	25	10
54	0.35	0.1	10000	0.35	10	25

support for practical multi-axis machining applications were obtained.

4.1 Variance and interactions for surface roughness

Variance analysis for surface roughness (SR) under down milling is shown in Table 2. The significance test of the model $P < 0.05$ indicates that the model is statistically significant. Lack of Fit item is used to represent the fitting degree between the model and the experimental data, namely the difference degree. In this case, the P value is $0.265 > 0.05$, the model is good, and there is no missing elements. Therefore, the practical test points in experimental results could be analyzed by the regression equation. Based on the analysis of variance of surface roughness, the model is significant, while the Lack of Fit item was not significant. Therefore, the regression Eq. (1) accurately expresses the relationship between the index and the process parameters.

According to Table 2, the response surface with two-factor interaction for surface roughness by eliminating the insignificant factors and retaining various significant factors is presented in Fig. 10.

$$\begin{aligned} Ra = {} & 250.97689 - 417.94722a_p - 1508.41995a_e + 0.16338n - 247.78333f_z \\ & - 44.14248tilt + 30.08416lead + 14.74778a_p{\cdot}lead - 1471.22222a_e{\cdot}f_z + \\ & 27.54611a_e{\cdot}tilt + 43.74222a_e{\cdot}lead - 5.89606E{-}003n{\cdot}lead + 19.83611f_z{\cdot}tilt \\ & + 0.57789tilt{\cdot}lead + 3658.71212a_e{}^2 + 0.22971tilt^2 + 0.15867lead^2 \end{aligned} \quad (1)$$

According to the diagnostics analysis of surface roughness, normal probability distribution of residuals is on a straight line. The distribution of data is linear and no abnormal data points appear. The regression model fits well (Fig. 8).

Also, the comparisons between the predicted values and the actual values of surface roughness were carried out, and the predicted values match well with the actual values, which is shown in the following Fig. 9 and Table 3. The residual distribution conditions show that the model is accurate.

According to response surface of surface roughness under down milling presented in Fig. 10, it could be found that combinations of smaller positive lead angle and larger depth of cut are conducive to get smaller surface roughness, and the combinations are also beneficial to improve the material removal rate. The machining system rigidity would be reduced when larger positive lead angles are adopted, which furtherly induce cutter deformation and the negative impact of adverse factors such as the system vibration. Hence, usage of larger positive *lead* should be avoided. By considering both the efficiency and surface quality, a_e should be decreased together with increasing f_z under the premise that the cutter performance is reliable when f_z is interacting with a_e.

For the interaction of either *tilt* and a_e or *lead* and a_e, it is found that smaller a_e together with larger positive *tilt* or larger positive *lead* should be preferred, because decreasing a_e would lead to the decrease of scallop height in cross-feed direction, and

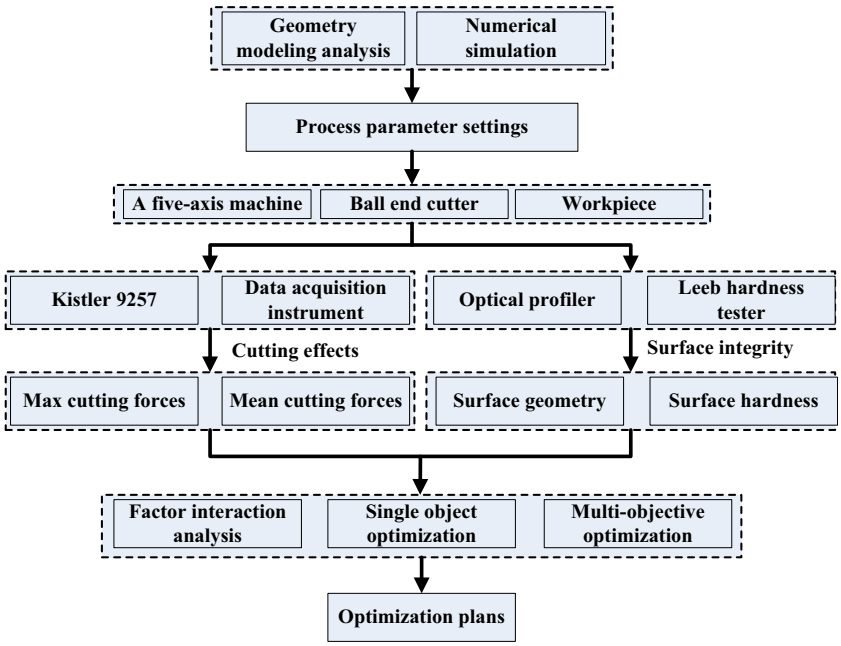

Fig. 6 Flow chart of the experimental design and optimization analysis

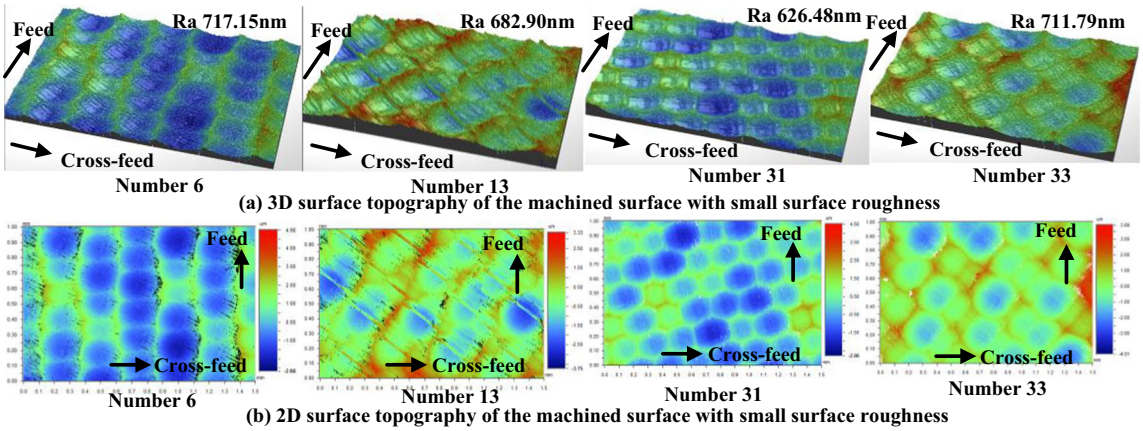

Fig. 7 Surface topography of the machined surface (down milling)

also increment of positive *tilt* or positive *lead* is beneficial to improve the residual materials in feed direction. In general, chip thickness changes from thick to thin, and considerable impact and rough surface would be induced if larger spindle speed is adopted. Hence, combinations of smaller positive *lead* and small *n* could induce smaller surface roughness when *lead* is interacting with spindle speed. Larger positive *tilt* and large f_z would be advantageous to obtain smaller surface roughness and high machining efficiency under the interaction of positive *tilt* and f_z.

Through the analysis of the interaction between *tilt* and *lead*, it is found that the ideal surface roughness can be obtained by the combination of larger positive *tilt* and smaller positive *lead*, and smaller values for both positive *tilt* and positive *lead* should be avoided because of the low effective cutting speed and unsatisfactory chip removal characteristics. At the range with smaller positive *lead*, surface roughness decreases with the increasing *tilt*, because the machining characteristics corresponding to larger *tilt* tend to represent the advantage under general down milling condition, which is beneficial to improve the surface finish.

Table 2 Variance analysis of SR prediction (down milling)

Source	Sum of squares	Degree of freedom	Mean square	*F* value	*P* value Prob > *F*	
Model	2.24E+ 06	16	1.40E+ 05	12.29	< 0.0001	Significant
A-a_p	1309.95	1	1309.95	0.11	0.7367	
B-a_e	1.36E+ 06	1	1.36E+ 06	119.37	< 0.0001	
C-*n*	13793.3	1	13793.3	1.21	0.2787	
D-f_z	7735.37	1	7735.37	0.68	0.4156	
E-*tilt*	1.04E+ 05	1	1.04E+ 05	9.08	0.0046	
F-*lead*	3096.74	1	3096.74	0.27	0.6055	
AF	8808.63	1	8808.63	0.77	0.3853	
BD	8766.2	1	8766.2	0.77	0.3864	
BE	61461.85	1	61461.85	5.39	0.0259	
BF	77491.97	1	77491.97	6.79	0.0131	
CF	2.82E+ 05	1	2.82E+ 05	24.68	< 0.0001	
DE	15935.59	1	15935.59	1.4	0.2448	
EF	1.35E+ 05	1	1.35E+ 05	11.85	0.0014	
B^2	74544.26	1	74544.26	6.53	0.0148	
E^2	29384.47	1	29384.47	2.58	0.1171	
F^2	16021.85	1	16021.85	1.4	0.2436	
Residual	4.22E+ 05	37	11410.69			
Lack of Fit	3.89E+ 05	32	12144.66	1.81	0.265	Not significant
Pure Error	33566.64	5	6713.33			
Cor Total	2.67E+ 06	53				

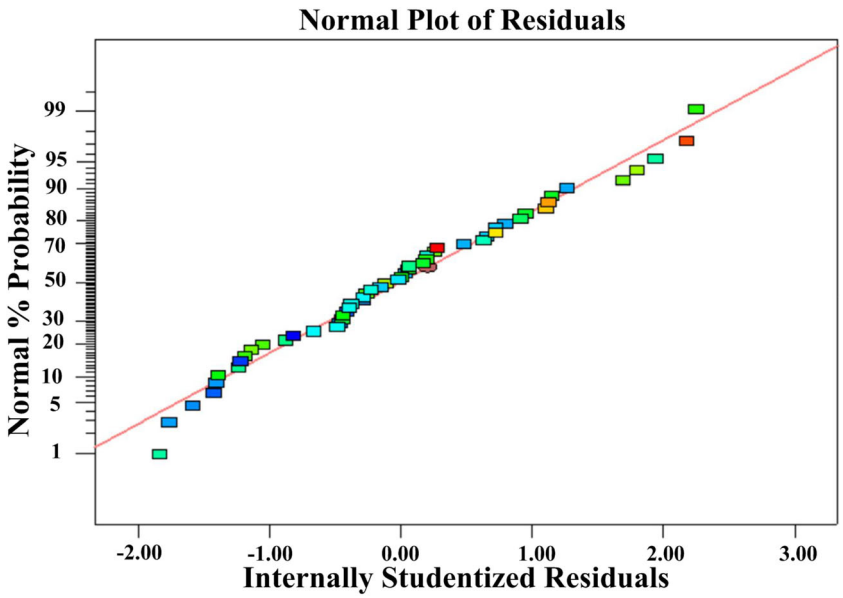

Fig. 8 Normal plot of residuals for surface roughness Ra

While at the range with larger positive *lead*, variation of surface roughness with the increasing *tilt* is not apparent.

4.2 Optimization for minimum SR

Taking two factors with the most significant interactions and ideal degree as the horizontal coordinate and ordinate, respectively, the surface response optimization results shown in Fig. 11 could be obtained under down milling condition. When other parameters are fixed at the optimal results, it is expected that the combination of large a_p and small positive *lead* will result in a smaller surface roughness according to the optimization results that aim to minimize surface roughness.

Table 4 shows the alternative optimized process plans with a high ideal degree for surface roughness, and the valuable recommendation plans for the machining strategy can be determined by combining actual machine tools, tools, and specific technical requirements.

5 Response and optimization of physical and mechanical indicators

5.1 Response and optimization of surface hardness

5.1.1 Variance and interactions analysis for SH

For surface roughness and hardness, the results of test of significance and variance analysis showed that the model was

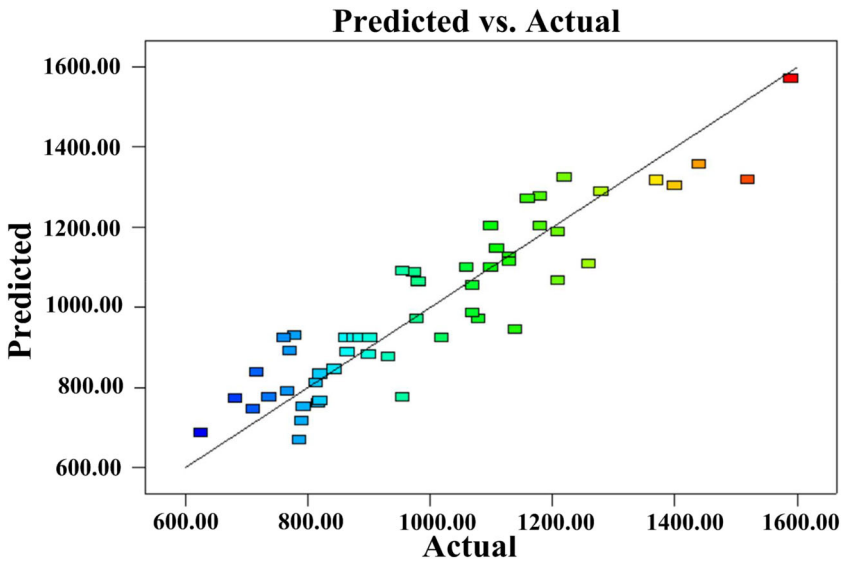

Fig. 9 The predicted and the actual values of SR (unit/nm)

Table 3 Diagnostics case statistics for surface roughness Ra

Standard order	Actual value	Predicted value	Residual	Leverage	Internally studentized residual	Externally studentized residual
1	818.52	761.5444	56.9756	0.3460	0.6595	0.6544
2	711.79	746.7686	− 34.9786	0.3460	− 0.4049	− 0.4003
3	1400	1304.2144	95.7856	0.3460	1.1088	1.1123
4	1280	1289.4386	− 9.4386	0.3460	− 0.1093	− 0.1078
5	767.63	791.8436	− 24.2136	0.3460	− 0.2803	− 0.2768
6	737.5	777.0678	− 39.5678	0.3460	− 0.4580	− 0.4531
7	1180	1202.1036	− 22.1036	0.3460	− 0.2559	− 0.2526
8	1210	1187.3278	22.6722	0.3460	0.2624	0.2591
9	863.63	924.7050	− 61.0750	0.2456	− 0.6583	− 0.6531
10	1180	1277.2125	− 97.2125	0.2456	− 1.0478	− 1.0492
11	1080	972.6517	107.3483	0.2456	1.1570	1.1625
12	1220	1325.1592	− 105.1592	0.2456	− 1.1334	− 1.1379
13	787.37	669.3300	118.0400	0.2456	1.2722	1.2833
14	1160	1269.7525	− 109.7525	0.2456	− 1.1829	− 1.1895
15	791.44	717.2767	74.1633	0.2456	0.7993	0.7954
16	1520	1317.6992	202.3008	0.2456	2.1804	2.3038
17	814.64	810.8764	3.7636	0.2418	0.0405	0.0399
18	1130	1124.1456	5.8544	0.2418	0.0629	0.0621
19	955.75	774.9706	180.7794	0.2418	1.9436	2.0232
20	973.73	1088.2397	− 114.5097	0.2418	− 1.2311	− 1.2400
21	1100	1098.9172	1.0828	0.2418	0.0116	0.0115
22	900.62	881.5414	19.0786	0.2418	0.2051	0.2024
23	981.79	1063.0114	− 81.2214	0.2418	− 0.8732	− 0.8703
24	844.49	845.6356	− 1.1456	0.2418	− 0.0123	− 0.0121
25	1130	1112.5832	17.4168	0.3460	0.2016	0.1990
26	1060	1097.8073	− 37.8073	0.3460	− 0.4376	− 0.4328
27	1070	987.4148	82.5852	0.3460	0.9560	0.9548
28	978.38	972.6390	5.7410	0.3460	0.0665	0.0656
29	771.22	891.9032	− 120.6832	0.3460	− 1.3970	− 1.4158
30	932.05	877.1273	54.9227	0.3460	0.6358	0.6306
31	1140	945.2598	194.7402	0.3460	2.2542	2.3940
32	778.7	930.4840	− 151.7840	0.3460	− 1.7570	− 1.8102
33	1100	1201.4639	− 101.4639	0.5297	− 1.3850	− 1.4030
34	1440	1357.1314	82.8686	0.5297	1.1312	1.1356
35	626.48	686.0389	− 59.5589	0.5297	− 0.8130	− 0.8092
36	955.53	1089.6214	− 134.0914	0.5297	− 1.8304	− 1.8932
37	820.69	767.2922	53.3978	0.5297	0.7289	0.7242
38	1370	1316.6397	53.3603	0.5297	0.7284	0.7237
39	682.9	771.9672	− 89.0672	0.5297	− 1.2158	− 1.2240
40	1590	1569.2297	20.7703	0.5297	0.2835	0.2800
41	820.75	833.4939	− 12.7439	0.3668	− 0.1499	− 0.1479
42	793.84	752.3531	41.4869	0.3668	0.4881	0.4830
43	1110	1146.7631	− 36.7631	0.3668	− 0.4325	− 0.4277
44	1210	1065.6222	144.3778	0.3668	1.6985	1.7448
45	1070	1055.1697	14.8303	0.3668	0.1745	0.1722
46	1260	1106.7589	153.2411	0.3668	1.8028	1.8619
47	717.15	837.7939	− 120.6439	0.3668	− 1.4193	− 1.4397
48	865.7	889.3831	− 23.6831	0.3668	− 0.2786	− − 0.2751
49	886.64	925.2176	− 38.5776	0.0657	− 0.3736	− 0.3692
50	1020	925.2176	94.7824	0.0657	0.9179	0.9159
51	875.78	925.2176	− 49.4376	0.0657	− 0.4788	− 0.4737
52	885.3	925.2176	− 39.9176	0.0657	− 0.3866	− 0.3821
53	902.3	925.2176	− 22.9176	0.0657	− 0.2220	− 0.2191
54	762.37	925.2176	− 162.8476	0.0657	− 1.5771	− 1.6108

statistically significant when model significance test $P < 0.05$ in Table 2 and Table 5.

The "Lack of Fit" term is used to represent the degree of fitting between the model and the experiment, that is, the degree of difference between them. According to the analysis of variance, P value is larger than 0.05, which means the "Lack of Fit" term is not significant, and there is no dissimulation factor exists. The relationship between the significant process parameters and surface hardness could be expressed by the corresponding three-time polynomial in six variables, as shown in Eq. (2), and it further indicates that the model fits well. Hence, the function could accurately represent the

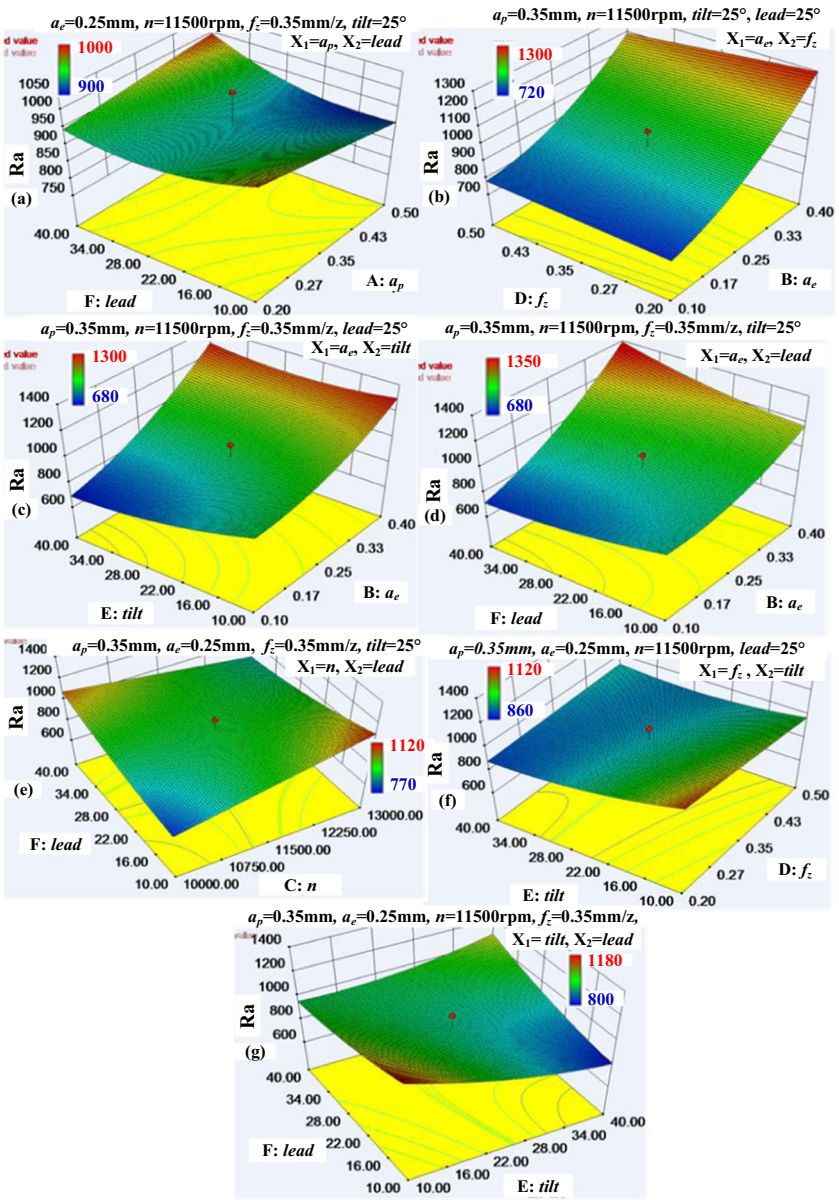

Fig. 10 SR of two-factor interactions under down milling **a** a_p and *lead,* **b** a_e and f_z, **c** n and *tilt,* **d** n and *lead,* **e** f_z and *lead,* and **f** *tilt* and *lead*

relation, and contributions of the single process parameter and a couple of factors with significant interaction are included in the fitting function.

$$Hl = +692.30641 - 123.78473a_p + 54.90547a_e - 1.36116E{-}003n - 1.56289a_e{\cdot}tilt + 7.02799E{-}004n{\cdot}f_z + 393.67487a_p^2 - 0.016337a_p^2{\cdot}n + 3.45902E{-}009n^2{\cdot}tilt \quad (2)$$

Figure 12 presents the interaction condition of the significant process factors for the machined surface hardness. The combinations of smaller positive *lead* and larger a_e or combinations of larger f_z and approximately smaller spindle speed would promote to generate high surface hardness, and combinations of smaller a_e and smaller positive *tilt* should be avoided. However, the increment of a_e would result in worse surface geometric features if high surface finish is required in

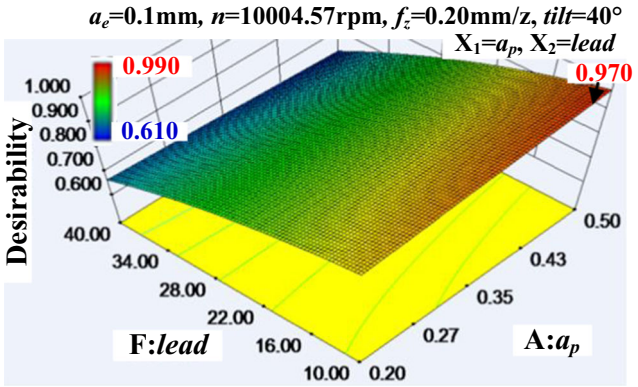

Fig. 11 Optimization results for minimum SR (down milling)

Table 4 Optimization plans for minimum SR (down milling)

Number	a_p /mm	a_e/ mm	n/(r/min)	f_z/(mm/ z)	*tilt*/°	*lead*/ °	*Ra*/nm	Desirability
1	0.48	0.1	10004.57	0.2	40	10	435.826	0.97
2	0.47	0.1	10000.03	0.23	40	10	449.836	0.958
3	0.45	0.1	10000	0.22	39.69	10	454.005	0.955
4	0.42	0.1	10000.85	0.21	39.93	10	454.2	0.954
5	0.46	0.11	10000.01	0.25	40	10	462.948	0.947
6	0.47	0.14	10000	0.2	39.62	10.04	466.284	0.944
7	0.4	0.1	10007.61	0.2	39.95	11.66	471.345	0.94
8	0.5	0.1	10000.47	0.2	36.44	10.67	484.191	0.929
9	0.43	0.16	10029.76	0.2	40	10	487.494	0.926
10	0.48	0.1	10007.58	0.34	39.93	10	492.343	0.922

the specific machining application. Coordination of process parameters should be determined by considering actual machining requirements.

When feed per tooth interacts with spindle speed, surface hardness decreases with the increasing spindle speed at high f_z, while the variation of surface hardness with spindle speed at low f_z is not significant. Combinations of high spindle speed and high f_z not only increase the surface hardness, but also greatly improve the materials removal rates. Surface hardness decreases with the increment of f_z at the range of high spindle speed, while increases with the increasing f_z at the range with low spindle speed. The machined surface hardness is closely related with the degree of grain refinement of the surface layer materials, which is apparently affected by the cutting heat and mechanical loads generated during the multi-axis machining process.

The interactions of the significant factors with three times are shown in Fig. 13, application of combinations of larger positive tilt angle and lower spindle speed could generate high surface hardness, and adjustment of tilt angle that plays an important in the formation mechanism of surface hardness greatly affects cutting postures of the engaged cutting edges and cutting performance. Combinations of higher spindle speed and larger depth of cut are beneficial to increase surface hardness, while the carrying capacity of the cutting tool and high speed performance of the machine tool should be seriously considered when using this kind of combinations in order to ensure tool life and cutting process safety.

5.1.2 Optimization for maximum SH

The optimized response surface for maximum surface hardness (SH) is presented in Fig. 14 and Table 6, and the ideal degree response is presented by treating significant factors

Table 5 Variance analysis of SH prediction (down milling)

Source	Sum of squares	Degree of freedom	Mean square	F value	P value prob > *F*	
Model	1655.22	8	206.9	2.61	0.0193	Significant
A-a_p	222.04	1	222.04	2.81	0.1009	
B-a_e	135.37	1	135.37	1.71	0.1976	
C-n	315.06	1	315.06	3.98	0.0521	
BE	144	1	144	1.82	0.1841	
CD	242	1	242	3.06	0.0872	
A^2	281.11	1	281.11	3.55	0.0659	
A^2C	315.19	1	315.19	3.98	0.052	
C^2E	231.13	1	231.13	2.92	0.0944	
Residual	3561.32	45	79.14			
Lack of fit	2753.32	40	68.83	0.43	0.9416	Not significant
Pure error	808	5	161.6			
Cor total	5216.54	53				

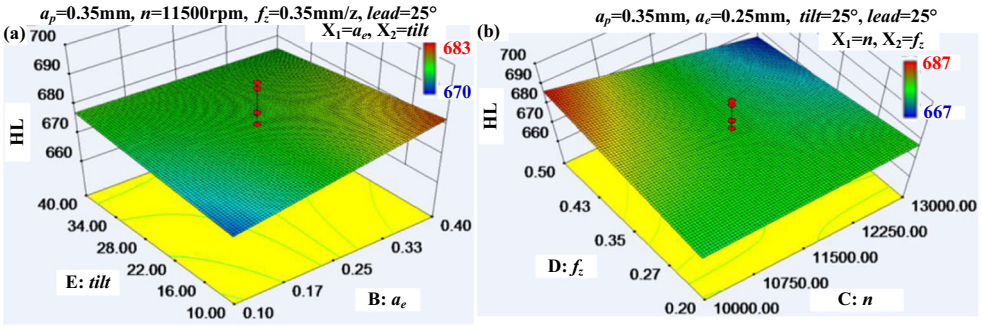

Fig. 12 SH with two-factor interactions under down milling **a** a_e and *tilt,* and **b** n and f_z

with great interaction as horizontal coordinate together with the other process parameters at an optimal value. It is found that a_p greatly affects surface hardness, and combinations of larger or smaller a_p and various positive *lead*, especially combinations of larger a_p and larger *lead*, could produce large ideal degree which corresponds to high surface hardness.

5.2 Response and optimization of the cutting forces

5.2.1 Variance and interactions analysis for average and maximum CF

The cutting forces significantly affect the cutting deformation, energy consumption, and tool life. In general, it is expected to produce small average or small maximum cutting forces (CF), which can achieve processing stability, improved energy consumption, and better tool life. The variance analysis for the average and the maximum CF response surface under down milling is shown in Table 7 and Table 8. The regression relationship between the CF and the process parameters could be represented by quadratic polynomial Eqs. (3) and (4).

$$\begin{aligned} Meanforces = {} & -71.21157 + 171.12963a_p + 118.38889a_e + 9.78611E{-}003n{-}26.16667f_z \\ & +3.54750tilt + 0.66000lead{-}170.00000a_p{*}a_e + 3.91667a_p{*}tilt{-}2.82222a_p{*}lead \\ & -0.015611a_e{*}n + 176.66667a_e{*}f_z + 2.27778a_e{*}lead{-}2.50556E{-}004n{*}tilt \\ & -2.62778f_z{*}tilt + 1.92222f_z{*}lead{-}0.040889tilt{*}lead{-}204.62963a_p{}^2 \end{aligned} \quad (3)$$

$$\begin{aligned} Maxforces = {} & -185.04155 + 985.94213a_p + 723.30787a_e + 0.011475n + 119.36111f_z \\ & +12.02750tilt{-}0.71333lead{-}585.00000a_p{\cdot}a_e{-}5.94444a_p{\cdot}lead \\ & -4.03333a_e{\cdot}tilt{-}1.20278E{-}003n{\cdot}tilt + 4.97222E{-}004n{\cdot}lead \\ & +7.19444f_z{\cdot}tilt{-}9.61111f_z{\cdot}lead{-}929.00463a_p{}^2{-}657.61574a_e{}^2 \end{aligned} \quad (4)$$

The interaction of significant factors for the average and maximum CF are presented in Fig. 15 and Fig. 16, respectively. The interactions between a_p and *tilt* or a_p and *lead* are both apparent with regard to the average cutting forces, and combinations of smaller a_p and larger positive *tilt* or combinations of smaller a_p and smaller positive *lead* help to apparently decrease the average cutting force. Selection of large tool inclination angles means to increase the effective cutting speed, and the maximum cutting force could be lowered by cooperating with smaller geometric characteristic parameters. According to Fig. 15 c, d, and e, it is found that combinations of small a_e and approximately low n or large positive *lead* or large f_z help to reduce the average cutting force. Machining with low n and small *tilt* would tend to produce small average CF, while the increment of spindle speed affects the stability of machining system at the range of high-speed cutting with small *tilt*, which would lead to the increasing average cutting force. However, the average cutting force decreases with the increasing spindle speed when adopting larger positive *tilt*, as is shown in Fig. 15 f. The larger *tilt* could generate ideal cutting postures of the engaged cutting edges, which would produce larger effective cutting speed. As is presented in Fig. 15 g and h, combinations of smaller f_z and smaller positive *tilt* or larger positive *lead* tend to decrease the average cutting force, and smaller f_z should be preferably selected to decrease

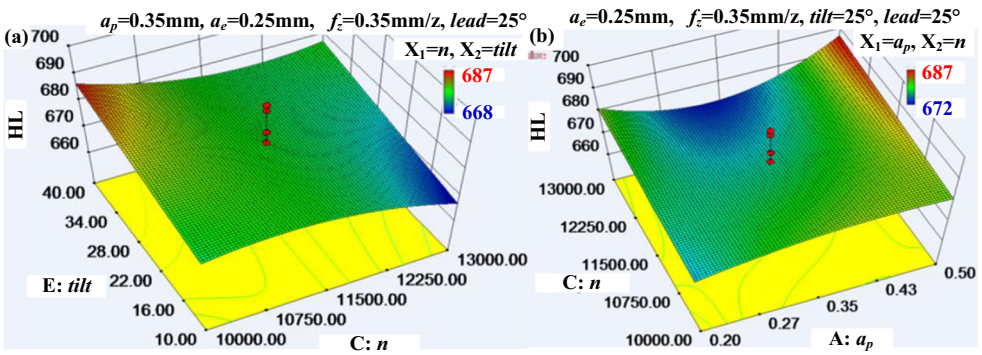

Fig. 13 SH with two-factor and three times interactions (down milling) **a** n^2 and *tilt,* and **b** $a_p{}^2$ and n

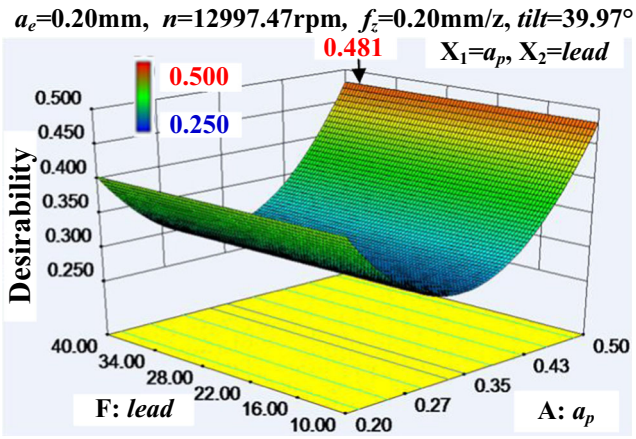

Fig. 14 Optimization results for maximum SH (down milling)

the initial cutting thickness that apparently influenced by f_z. Based on the analysis of the interaction presented in Fig. 15 i, both positive *lead* and positive *tilt* with larger or smaller values are conducive to reducing the average cutting force, while it is recommended to avoid using combinations of smaller positive *lead* and larger positive *tilt* to decrease the initial cutting thickness and average cutting force.

The maximum cutting forces are greatly affected by the vibration of the machining system, and are closely related with the materials' removal rates. According to the response surfaces presented in Fig. 16 a, b, and c, the geometric quantity in the process parameters, such as a_p or a_e, should keep in small values to achieve the decreasing maximum cutting force. Application of combinations of small *lead* and small a_p or combinations of small *tilt* and small a_e could apparently decrease the maximum cutting force. At the range with smaller a_p, the maximum cutting force increase with the increasing *lead*, while the maximum cutting force is slightly reduced at the range with larger a_p. The lead angle directly affects the initial cutting thickness, and also the effective cutting speed, the instantaneous tool-chip contact length, and the instantaneous uncut chip thickness are directly influenced by the variations of *lead*. At the range with smaller a_e, the maximum cutting force increases with the increasing *tilt*, while the maximum cutting force slightly decreases with the increasing *tilt* at the range with larger a_e. The *tilt* directly influences the tool-chip contact length and uncut chip thickness at the instants of time, and the combination of tool-chip and chip thickness would further affect the appearance moment of the maximum cutting force during the milling process.

The interaction between tool inclination angle and movement parameters in process system is presented in Fig. 16 d, e, f, and g. Combinations of larger *tilt* and high spindle speed or large *tilt* and small f_z would significantly decrease the maximum cutting force. Increasing *tilt* or spindle speed would directly increase the effective cutting speed, and the maximum cutting forces would decrease when the cutting speed reaches the range of high-speed cutting for this kind of workpiece materials. The uncut chip thickness and materials' removal rate increase with the increasing f_z, and further the chip load and mechanical load acting on the tool increase, which promote the increment of the maximum cutting force during the down milling process. Usage of combinations of smaller *lead* and high spindle speed or smaller f_z would apparently decrease the maximum cutting force to some extent, because the increment of *lead* would directly increase the initial cutting thickness and more intense mechanical impact under down milling condition.

5.2.2 Optimization for minimum average and maximum CF

Optimization response surface with minimum the average and maximum cutting force as single objective is presented in Fig. 17, and the two evaluation indicators are equally important in the optimization process. The interaction of *lead* and a_p significantly influences the cutting force

Table 6 Optimization plans for maximum SH (down milling)

Number	a_p/mm	a_e/mm	n/(r/min)	f_z/(mm/z)	$tilt$/°	$Lead$/°	Hardness/HL	Desirability
1	0.5	0.25	12997.47	0.2	39.97	38.08	698.476	0.481
2	0.5	0.28	12999.94	0.2	39.87	34.46	698.472	0.481
3	0.49	0.1	12999.03	0.2	40	16.14	698.303	0.479
4	0.49	0.1	12999.03	0.2	40	33.86	698.303	0.479
5	0.5	0.33	12999.62	0.2	39.99	10	698.224	0.478
6	0.49	0.21	13000	0.2	40	18.7	697.869	0.473
7	0.5	0.38	13000	0.2	38.39	37.05	697.78	0.472
8	0.5	0.1	12852.83	0.2	40	11.69	697.379	0.467
9	0.5	0.1	12852.83	0.2	40	38.31	697.379	0.467
10	0.5	0.27	13000	0.2	36.43	15.6	697.36	0.467

Table 7 Variance analysis of the average CF prediction (down milling)

Source	Sum of squares	Degree of freedom	Mean square	*F* value	*P* value prob > *F*	
Model	3348.47	17	196.97	2.14	0.0271	Significant
A-a_p	87.78	1	87.78	0.95	0.3352	
B-a_e	1.87	1	1.87	0.02	0.8874	
C-n	7.82	1	7.82	0.085	0.7723	
D-f_z	0.07	1	0.07	7.65E− 04	0.9781	
E-tilt	48.73	1	48.73	0.53	0.4715	
F-lead	62.73	1	62.73	0.68	0.4144	
AB	117.04	1	117.04	1.27	0.2669	
AE	621.28	1	621.28	6.75	0.0135	
AF	322.58	1	322.58	3.51	0.0693	
BC	98.7	1	98.7	1.07	0.3073	
BD	126.41	1	126.41	1.37	0.2489	
BF	210.12	1	210.12	2.28	0.1395	
CE	254.25	1	254.25	2.76	0.1051	
DE	279.66	1	279.66	3.04	0.0898	
DF	149.64	1	149.64	1.63	0.2104	
EF	677.12	1	677.12	7.36	0.0102	
A^2	282.64	1	282.64	3.07	0.0882	
Residual	3312.59	36	92.02			
Lack of fit	2932.05	31	94.58	1.24	0.4449	Not significant
Pure error	380.55	5	76.11			
Cor total	6661.06	53				

Table 8 Variance analysis of the maximum CF prediction (down milling)

Source	Sum of squares	Degree of freedom	Mean square	*F* value	*P* value prob > *F*	
Model	35537.28	15	2369.15	2.41	0.0144	Significant
A-a_p	897.93	1	897.93	0.91	0.3452	
B-a_e	4269.33	1	4269.33	4.34	0.0439	
C-n	2051.65	1	2051.65	2.09	0.1567	
D-f_z	1876.2	1	1876.2	1.91	0.1752	
E-tilt	469.05	1	469.05	0.48	0.4939	
F-lead	1044.12	1	1044.12	1.06	0.3092	
AB	1386.01	1	1386.01	1.41	0.2424	
AF	1431.13	1	1431.13	1.46	0.235	
BE	1317.69	1	1317.69	1.34	0.2542	
CE	5859.03	1	5859.03	5.96	0.0194	
CF	2002.56	1	2002.56	2.04	0.1616	
DE	2096.28	1	2096.28	2.13	0.1524	
DF	3741.13	1	3741.13	3.81	0.0585	
A2	5592.56	1	5592.56	5.69	0.0222	
B2	2802.33	1	2802.33	2.85	0.0995	
Residual	37351.62	38	982.94			
Lack of fit	34191.17	33	1036.1	1.64	0.3072	Not significant
Pure error	3160.45	5	632.09			
Cor total	72888.91	53				

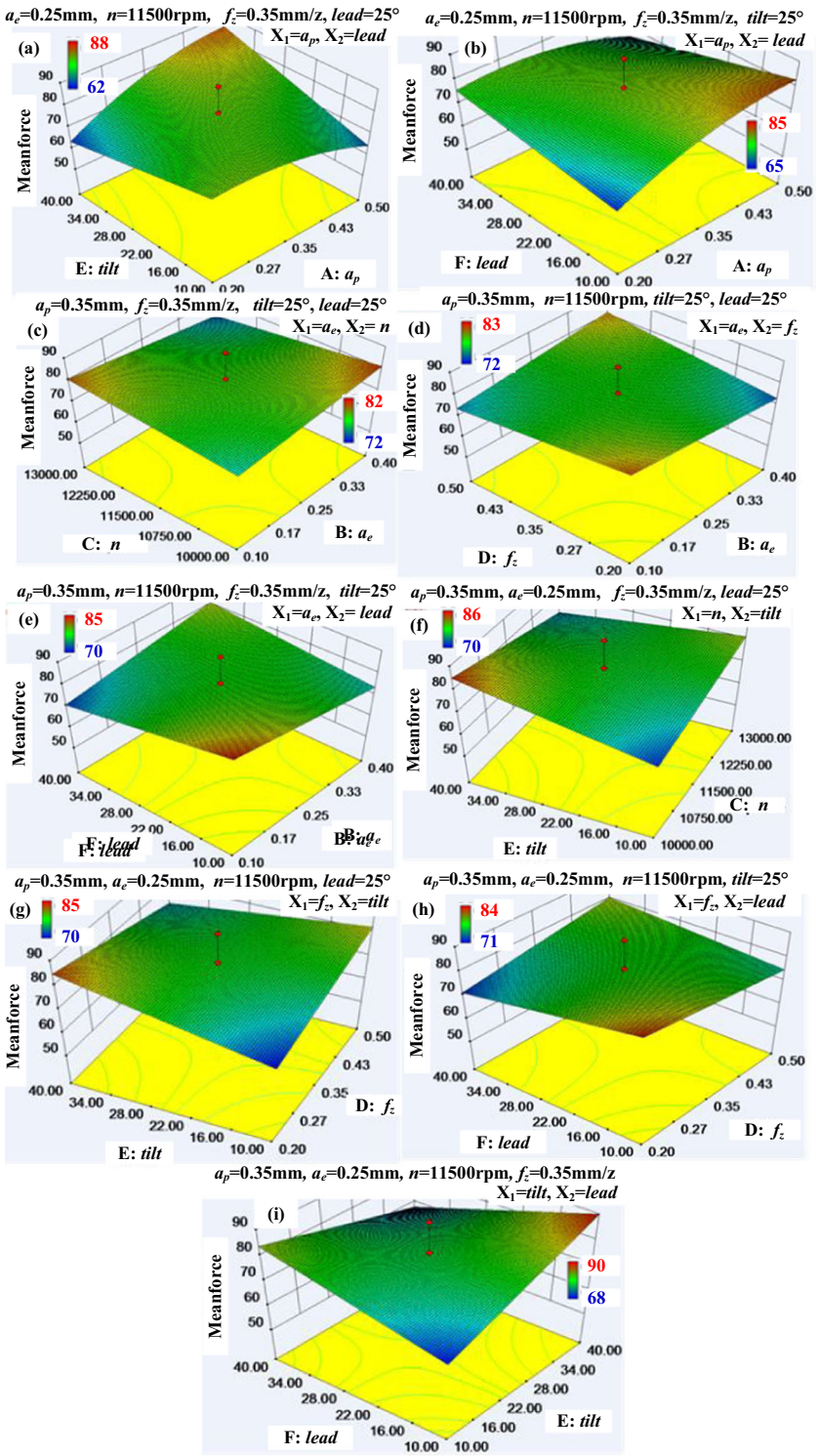

Fig. 15 Variations of the average CF with two-factor interactions (down milling) **a** a_p and *tilt*, **b** a_p and *lead*, **c** a_e and *n*, **d** a_e and f_z, **e** a_e and *lead*, **f** *n* and *tilt*, **g** f_z and *tilt*, **h** f_z and *lead*, and **i** *tilt* and *lead*

under down milling condition. Combinations of small *lead* and large a_p should be avoided to decrease the cutting forces generated during milling process, and combinations of large *lead* and small a_p are preferred for the purpose to decreasing the cutting forces. The cutting postures of the engaged cutting edges related to effective cutting speed corresponding to larger *lead* are conducive to improve the cutting performance during the down milling process. Table 9 shows the optimization plans for minimum average and maximum cutting force. The recommended process plans could be referenced for practical machining with the requirements of cutting forces control,

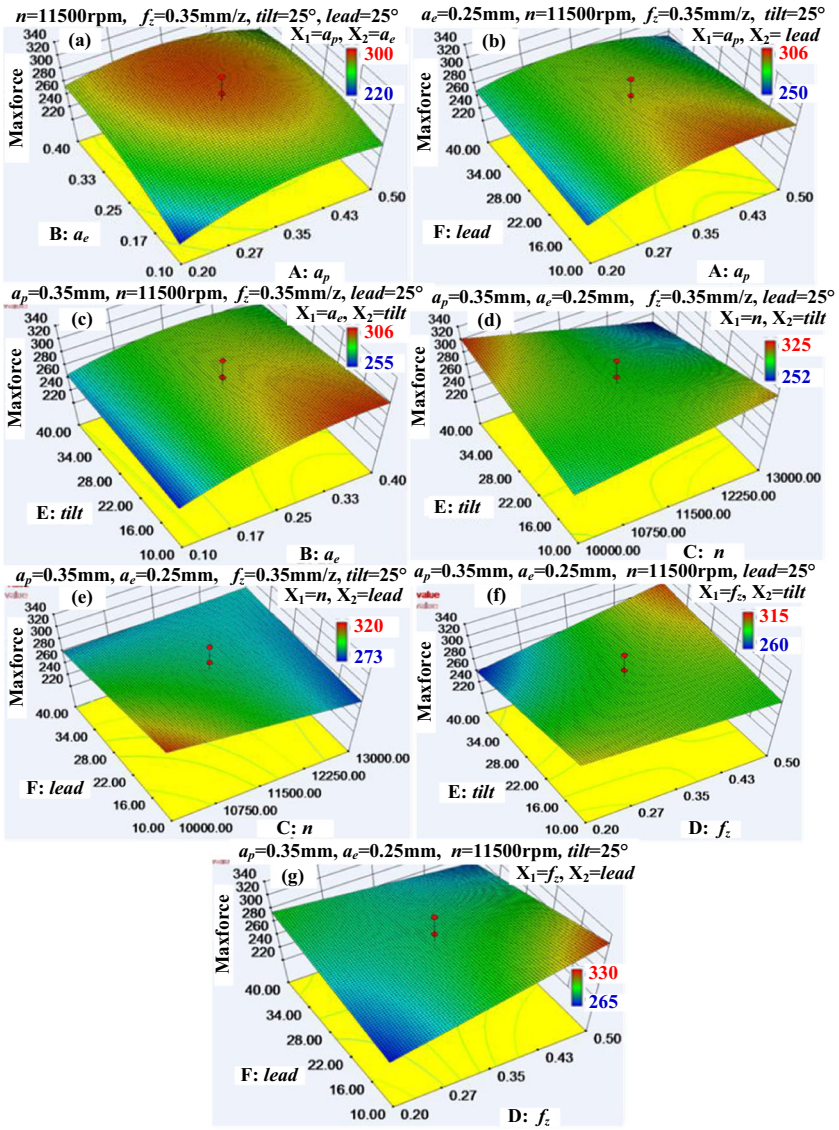

Fig. 16 Variations of the maximum CF of two-factor interactions (down milling) **a** a_p and a_e **b** a_p and *lead*, **c** a_e and *tilt*, **d** *n* and *tilt*, **e** *n* and *lead*, **f** f_z and *tilt*, and **g** f_z and *lead*

and the optimization plans could also be approximately modified on the basis of ensuring the machining reliability.

6 Multi-objective coupling optimization considering cutting effects and surface integrity

The process parameters were constrained in a certain range that covers the range of conventional process parameters' change domain before a multi-objective coordination optimization. Further, the optimization plans were refined in a more comprehensive process parameter range. The optimization with the comprehensive target of minimizing SR (weight 5), maximizing SH (weight 5), minimizing the average (weight 3), and the maximum CF (weight 3) is presented in Fig. 18 under down milling process. Combinations of small a_p and small a_e or combinations of large a_p and small a_e could lead to

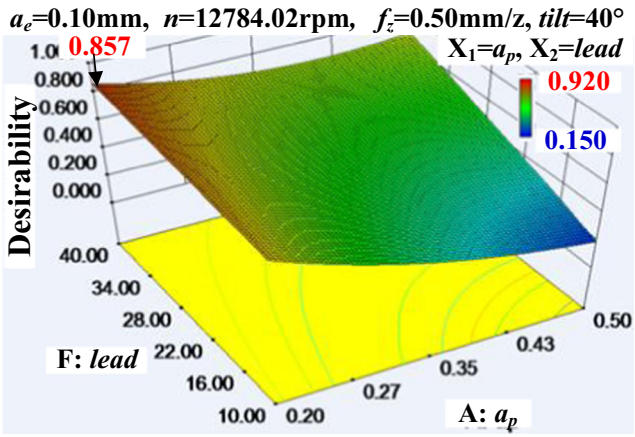

Fig. 17 Optimization results for minimum the average and maximum CF

Table 9 Optimization plans for minimizing the CF (down milling)

Number	a_p/mm	a_e/mm	n/(r/min)	f_z/(mm/z)	*tilt*/°	*lead*/°	Desirability
1	0.2	0.1	12784.02	0.5	40	39.45	0.857
2	0.2	0.1	12995.8	0.46	39.86	35.77	0.855
3	0.2	0.1	12999.83	0.36	40	33.67	0.839
4	0.2	0.1	12977.71	0.46	39.98	30.19	0.836
5	0.2	0.1	12713.64	0.38	40	39.8	0.834
6	0.21	0.11	12999.69	0.47	39.65	40	0.832
7	0.22	0.1	12742.82	0.5	40	39.37	0.829
8	0.2	0.1	12841.97	0.45	39.85	29.53	0.825
9	0.2	0.1	12870.64	0.4	39.02	29.8	0.813
10	0.2	0.1	12408.22	0.47	40	29.42	0.792

high ideal degree when adopting larger tool inclination angles, smaller f_z, and high spindle speed for multi-objective optimization. The a_e significantly affects the ideality because the surface scallop height in the cross-feed direction increases as the a_e increases, which produces a rough surface. However, a_P does not result in adverse effects to the machined surface if only geometrical analysis based on the movement characteristics of the engaged cutting edges is considered for finish machining. Combinations of large *lead*, large *tilt*, and high spindle speed that will increase the cutting speed would give full play to the advantage of high-speed cutting. Multi-objective coupling optimizations that take into account the combined effects of reasonable machining process and surface integrity assessment indicators can be provided to support specific applications.

The importance degrees of SR, SH, average, and maximum CF are set as 5/16, 5/16, 3/16, and 3/16, respectively. The process parameters are restrained in the recommended range, and the upper and lower fluctuation values of evaluation indicators would affect ideal degree values. Multi-objective coordinated optimization plans could be concluded in accordance with reasonable upper and lower fluctuation values for evaluation indicators, as is shown in Table 10.

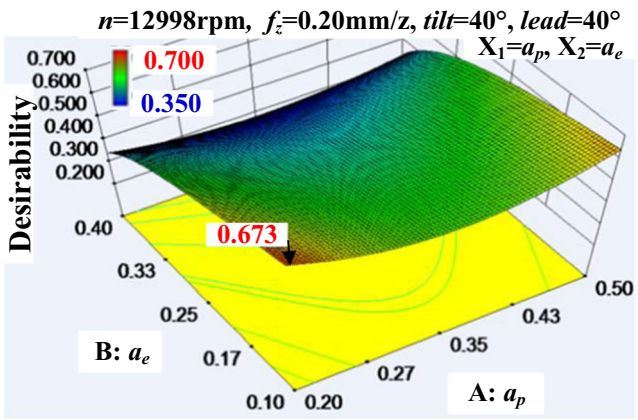

Fig. 18 Ideal degree of multi-objective coordinated optimization (down milling)

7 Conclusions

(1) In some works, the theoretical analytical models were established to predict roughness and cutting force, and the model is constructed from the geometric and physical levels by combining with the empirical coefficient of actual cutting test. The surface hardness that is related to the microstructure of the machined metamorphic layer, heat-affected zone, and process parameters is difficult to predict in analytical methods. There are some equivalent treatments, which will generate error sources and cause great difficulty. Five-axis ball end milling at high speed is complicated, and the thermal mechanical coupling, vibration, deformation, and friction in the machining system will have certain influence on the prediction results, which has important theoretical significance and value.

Based on a large number of experimental data, this work carried out statistical analysis, such as variance analysis, model significance test, and residual diagram, to a certain extent to ensure the effectiveness and accuracy of the prediction model, and can predict the cutting effects and machining quality of five-axis high-speed ball end milling within a certain range. At the same time, the optimization targets were set, and the corresponding optimization schemes of five-axis high-speed ball end milling of hardened steel were obtained, which has strong operability and good practical application value for advanced manufacturing technology.

(2) The machining characteristics, chip formation process, and the milled surface formation were discussed. Under down milling condition, the analysis of variance and interaction of significant factors for surface integrity and cutting forces were discussed, and the polynomial equations reflecting

Table 10 Multi-objective optimization plans (down milling)

Number	a_p/mm	a_e/mm	n/(r/min)	f_z/(mm/z)	*tilt*/°	*lead*/°	Desirability
1	0.2	0.1	12998.62	0.2	40	40	0.673
2	0.2	0.1	12980.62	0.21	39.95	32.16	0.659
3	0.2	0.1	13000	0.3	39.98	40	0.649
4	0.2	0.1	13000	0.31	39.68	40	0.644
5	0.2	0.1	13000	0.33	39.99	35.41	0.637
6	0.2	0.16	12999.97	0.2	40	38.07	0.637
7	0.5	0.1	12999.97	0.23	39.55	40	0.634
8	0.5	0.1	13000	0.22	40	40	0.631
9	0.2	0.1	12689.35	0.24	40	40	0.628
10	0.5	0.13	12999.99	0.2	40	40	0.626
11	0.2	0.1	12995.33	0.32	39.91	27.89	0.625
12	0.21	0.11	12752.85	0.2	40	39.31	0.624
13	0.2	0.1	12551.31	0.23	40	37.68	0.618
14	0.49	0.15	12999.97	0.2	40	39.98	0.616
15	0.49	0.1	13000	0.26	39.98	40	0.616
16	0.5	0.14	12998.91	0.25	39.92	39.97	0.616
17	0.5	0.12	12995.78	0.31	39.98	40	0.614
18	0.5	0.1	12991.66	0.25	40	36.84	0.612
19	0.5	0.12	12995.23	0.2	34.78	39.67	0.609
20	0.23	0.11	12999.99	0.21	40	28.95	0.609
21	0.2	0.1	13000	0.25	40	21.01	0.604
22	0.47	0.1	12997.53	0.24	39.99	39.95	0.604
23	0.2	0.11	12999.98	0.2	32.5	30.87	0.597
24	0.2	0.1	12999.74	0.21	37.61	20.35	0.591
25	0.5	0.1	12872.11	0.25	32.91	40	0.591

the relationship between the evaluation indicators and machining parameters were obtained.

(3) The effective cutting speed and material removal characteristics are ideal under positive *tilt*, positive *lead*, and combinations of positive *tilt* and positive *lead* for down milling condition, and the uncut chip materials could be smoothly removed along the chip pocket without squeezing the final machined surface especially when adopting combinations of positive *tilt* and positive *lead*.

(4) For optimization of surface roughness under down milling condition, combinations of large a_p and small positive *lead* are ideal process plans when other parameters are fixed at optimal values. Depth of cut significantly affects the machined surface hardness under down milling condition, and application of large or small a_p and various positive lead angles could result in high ideal degree of surface hardness optimization. The interaction between *lead* and a_p apparently affects the cutting forces, and small positive *lead* and large a_p are suggested to be avoided to decrease the cutting forces, while combinations of large *lead* and small a_p would be the preferred coordinated process factors.

(5) Combinations of small a_p and small a_e or combinations of large a_p and small a_e could lead to high ideal degree when adopting larger tool inclination angles, small f_z, and high spindle rotation speed for multi-objective optimization. Combinations of larger *lead*, large *tilt*, and high spindle rotation speed could give full play to the advantage of high-speed cutting technology. The process optimization plans could be comprehensively considered to realize the ideal machining effects and better surface quality according to the practical application requirements.

(6) Due to the complexity of the multi-axis ball end milling process at high speed, it is urgent to improve processing quality and efficiency from the perspective of process strategy optimization, and there also needs to further improve the basic research and application problems from multi-axis customized modeling simulation and high-speed machining error compensation, tool wear and tool life optimization, research and development of multi-axis machining tool for specific difficult-to-cut materials, and strategies to reduce the overall processing energy consumption in order to promote engineering optimization application of this technology.

Funding information This work is supported by the National Natural Science Foundation of China (51505468), the Science and Technology Development Program of Shandong Province (2014GGX103041), and the National Basic Research Program of China (2009CB724402).

References

1. Lazoglu I, Boz Y, Erdim H (2011) Five-axis milling mechanics for complex free form surfaces. CIRP Ann Manuf Technol 60(1):117–120
2. Dudzinski D, Devillez A, Moufki A, Larrouquère D, Zerrouki V, Vigneau J (2004) A review of developments towards dry and high speed machining of Inconel 718 alloy. Int J Mach Tools Manuf 44(4):439–456
3. Yan H, Qian G, Hu Q (2007) Development of flow stress of AISI H13 die steel in hard machining. J Wuhan Univ Technol 22(2):187–190
4. Toh CK (2004) Surface topography analysis in high speed finish milling inclined hardened steel. Precis Eng 28(4):386–398
5. Daymi A, Boujelbene M, Ben Amara A, Bayraktar E, Katundi D (2011) Surface integrity in high speed end milling of titanium alloy Ti-6Al-4V. Mach Sci Technol 27(1):387–394
6. Axinte DA, Dewes RC (2002) Surface integrity of hot work tool steel after high speed milling-experimental data and empirical models. J Mater Process Technol 127(3):325–335
7. Mhamdi MB, Boujelbene M, Bayraktar E, Zghal A (2012) Surface integrity of titanium alloy Ti-6Al-4 V in Ball end Milling. Phys Procedia 25:355–362
8. Pu Z, Singh A (2013) High speed ball nose end milling of hardened AISI A2 tool steel with PCBN and coated carbide tools. J Manuf Process 15(4):467–473
9. Denkena B, Böß V, Nespor D, Samp A (2011) Kinematic and stochastic surface topography of machined TiAl6V4-Parts by means of ball nose end milling. Procedia Eng 19:81–87
10. Barakchi Fard MJ, Feng HY (2009) Effect of tool tilt angle on machining strip width in five-axis flat-end milling of free-form surfaces. Int J Adv Manuf Technol 44(3-4):211–222
11. Aspinwall DK, Dewes RC, Ng EG, Sage C, Soo SL (2007) The influence of cutter orientation and workpiece angle on machinability when high-speed milling Inconel 718 under finishing conditions. Int J Mach Tools Manuf 47(12–13):1839–1846
12. Guo DM, Ren F, Sun YW (2010) An approach to modeling cutting forces in five-axis ball-end milling of curved geometries based on tool motion analysis. J Manuf Sci Eng 132(4):575–590
13. Zhang L (2011) Process modeling and toolpath optimization for five-axis ball-end milling based on tool motion analysis. Int J Adv Manuf Technol 57(9-12):905–916
14. Becze CE, Clayton P, Chen L, El-Wardany TI, Elbestawi MA (2000) High-speed five-axis milling of hardened tool steel. Int J Mach Tools Manuf 40(6):869–885
15. Ozturk E, Budak E (2010) Dynamics and stability of five-axis ball-end milling. J Manuf Sci Eng 132(2):021003–021013
16. Ozturk E, Tunc LT, Budak E (2009) Investigation of lead and tilt angle effects in 5-axis ball-end milling processes. Int J Mach Tools Manuf 49(14):1053–1062
17. Chen X, Zhao J, Li Y, Han S, Cao Q, Li A (2012) Numerical modelling of high-speed ball end milling with cutter inclination angle. PIMechE Part B J Eng Manuf 226(4):606–616
18. Farouki RT, Li S (2013) Optimal tool orientation control for 5-axis CNC milling with ball-end cutters. Comput Aided Geom D 30(2):226–239
19. Sun Y, Bao Y, Kang K, Guo D (2013) A cutter orientation modification method for five-axis ball-end machining with kinematic constraints. Int J Adv Manuf Technol 67(9-12):2863–2874
20. Kalvoda T, Hwang Y-R (2009) Impact of various ball cutter tool positions on the surface integrity of low carbon steel. Mater Des 30(9):3360–3366
21. Chen X, Zhao J, Zhang W (2015) Influence of milling modes and tool postures on the milled surface for multi-axis finish ball-end milling. Int J Adv Manuf Technol 77(9-12):2035–2050
22. Chen X, Zhao J, Dong Y, Li A, Wang D (2014) Research on the machined surface integrity under combination of various inclination angles in multi-axis ball end milling. PIMechE, Part B: Journal of Engineering Manufacture. 228(1):31–50
23. Chen X, Zhao J, Dong Y, Han S, Li A, Wang D (2013) Effects of inclination angles on geometrical features of machined surface in five-axis milling. Int J Adv Manuf Technol 65(9-12):1721–1733
24. Kuram E, Ozcelik B (2013) Multi-objective optimization using Taguchi based grey relational analysis for micro-milling of Al 7075 material with ball nose end mill. Measurement. 46(6):1849–1864
25. Thepsonthi T, Özel T (2012) Multi-objective process optimization for micro-end milling of Ti-6Al-4V titanium alloy. Int J Adv Manuf Technol 63(9-12):903–914
26. Sivasakthivel PS, Velmurugan V, Sudhakaran R (2010) Prediction of vibration amplitude from machining parameters by response surface methodology in end milling. Int J Adv Manuf Technol 53(5-8):453–461